Chinese Physics Letters

中国物理学会 Chinese Physical Society

PAPER

Local Rotational Jamming and Multi-Stage Hyperuniformities in an Active Spinner System

To cite this article: Rui Liu *et al* 2023 *Chinese Phys. Lett.* **40** 126402

View the article online for updates and enhancements.

You may also like

- Dynamic evolution of hyperuniformity in a driven dissipative colloidal system
Ü Seleme Nizam, Ghaith Makey, Michaël Barbier et al.
- Microscopic theory for hyperuniformity in two-dimensional chiral active fluid
Yuta Kuroda and Kunimasa Miyazaki
- Multifunctional hyperuniform cellular networks: optimality, anisotropy and disorder
S Torquato and D Chen

This content was downloaded from IP address 159.226.35.241 on 28/12/2023 at 10:58

Chinese Physics Letters **40**, 126402 (2023) **Express Letter**

Local Rotational Jamming and Multi-Stage Hyperuniformities in an Active Spinner System

Rui Liu(刘锐)[1*], Jianxiao Gong(巩建晓)[2,4], Mingcheng Yang(杨明成)[1,3], and Ke Chen(陈科)[1,3]

[1]*Beijing National Laboratory for Condensed Matter Physics and CAS Key Laboratory of Soft Matter Physics, Institute of Physics, Chinese Academy of Sciences, Beijing 100190, China*
[2]*National Center for Nanoscience and Technology, Beijing 100190, China*
[3]*School of Physical Sciences, University of Chinese Academy of Sciences, Beijing 100049, China*
[4]*School of Nanoscience and Engineering, University of Chinese Academy of Sciences, Beijing 100049, China*

(Received 8 October 2023; accepted manuscript online 8 November 2023)

An active system consisting of many self-spinning dimers is simulated, and a distinct local rotational jamming transition is observed as the density increases. In the low density regime, the system stays in an absorbing state, in which each dimer rotates independently subject to the applied torque; while in the high density regime, a fraction of the dimers become rotationally jammed into local clusters, and the system exhibits microphase-separation like two-phase morphologies. For high enough densities, the system becomes completely jammed in both rotational and translational degrees of freedom. Such a simple system is found to exhibit rich and multiscale disordered hyperuniformities among the above phases: the absorbing state shows a critical hyperuniformity of the strongest class and subcritically preserves the vanishing density fluctuation scaling up to some length scale; the locally jammed state shows a two-phase hyperuniformity conversely beyond some length scale with respect to the phase cluster sizes; the totally jammed state appears to be a monomer crystal, but intrinsically loses large-scale hyperuniformity. These results are inspiring for designing novel phase-separation and disordered hyperuniform systems through dynamical organization.

DOI: 10.1088/0256-307X/40/12/126402

Disordered hyperuniform systems are exotic states of matter, which are isotropic as liquids or glasses but suppress long-wavelength density fluctuations as crystals.[1–5] Amorphous materials with density hyperuniformity are naturally endowed with superior physical properties[6–11] and are thus of great importance in both science and technology. Synthesis of hyperuniform amorphous materials is a double challenge, as crystallization needs to be avoided while hyperuniformity should not be hampered. Single-component synthesis, which provides the great advantage of easy manipulation, hardly produces both disorder and hyperuniformity, especially in low dimensions.

Active matter may be promising for tackling such a difficulty. First, active systems may form structures due to dynamical organization which may avoid crystallization even for a monodisperse constituent. Monodisperse self-spinning rods have been observed to form some disordered structures though not discussed in detail.[12,13] Second, active matter utilizes energy locally, and thus may prevent the formation of meta-stable local structures which would destroy density hyperuniformity. Many active systems thus exhibit density hyperuniformity without relying on long-range interactions as required in equilibrium systems.[1,14] Circle swimmer[15,16] and active spinner[17] systems have been shown to be density hyperuniform in their active fluidic regimes.

Here by employing the previously studied model,[13,17] we show that fast-spinning active dimers, not only undergo the previously reported jamming transition from an absorbing state (ABS) to an intermediate squeezed fluid and finally to a totally jammed state (TJS),[12,13] but also exhibit a distinct microphase-separation like feature that jamming happens locally and homogeneously. The intermediate fluidic state thus becomes a locally jammed state (LJS) exhibiting a two-phase morphology.

We identify that such an active spinner system in a critical ABS could also be both disordered and strongly hyperuniform, and the local jamming transition even leads to a two-phase hyperuniformity. The ABS is found to subcritically preserve the hyperuniformity density-fluctuation suppression up to some length scale, which diverges at the critical point. The intermediate LJS shows a hyperuniformity scaling beyond some length scale with respect to the phase cluster sizes. The final TJS appears to be a crystal for the constituent monomers of the dimers but an amorphous media for the dimer centroids, which suppresses density fluctuations as that in a strongly hyperuniform case at small length scales but shows a non-hyperuniform characteristic at large scales. To our knowledge, such a rich exhibition of multiscale hyperuniformities in a single system is rare.

We simulate a two-dimensional (2D) active spinner system as those described in Refs. [13,17]. Each spinner is a dimer consisting of two spherical monomers bonded with

*Corresponding author. Email: lr@iphy.ac.cn
© 2023 Chinese Physical Society and IOP Publishing Ltd

fixed length $\sigma = 1$ [Fig. 1(a)]. Each monomer has a mass $m = 1$ and each dimer has a moment of inertia $I = \frac{1}{2}m\sigma^2$. The monomers from different dimers interact with each other through a Weeks–Chandler–Andersen potential with a cutoff distance $r_c \equiv 2^{1/6}\sigma$. With the total effect of all such pair interactions denoted by $U(t)$, the dynamics of any dimer i is governed by

$$2m\ddot{\boldsymbol{r}}_i = -2\gamma_t\dot{\boldsymbol{r}}_i - \nabla_i U(t),$$
$$I\ddot{\theta}_i = \mathcal{T} - \gamma_s\dot{\theta}_i - \partial_{\theta_i}U(t),$$

where $\mathcal{T}$ is the driving torque, γ_t and γ_s are the translational and the rotational viscosities, respectively. All the simulation details are described in the Supplementary Information. Particularly, we choose a small γ_s to induce fast-spinning but a large γ_t to reduce diffusion. We thus have a large relaxation time ratio $\tau_s/\tau_t = 1000$, which is crucial for the jamming transition to occur locally. Typically, a system with N dimers in a square box of length L is simulated, and its number density is simply evaluated as $\phi = N\sigma^d/L^d$ (with the dimension $d = 2$).

With the above settings, all the mentioned states (ABS, LJS, and TJS) can be observed in the simulated system. First, the ABS, in which each dimer rotates independently subject to the applied torque, is observed for relatively low densities [Fig. 1(d)]. As the density increases, the system undergoes a local jamming transition and transits into an LJS. The main jamming feature observed at first is in the rotational degree of freedom that the involved dimers cease to spin freely and are compacted into local clusters. As the remaining dimers still keep spinning and are organized into relatively loose structures, a two-phase morphology develops [Fig. 1(f)]. For a very dense system, no dimer can diffuse and rotate any more, and the system gets totally jammed in all degrees of freedom (a TJS). The TJS appears to be an imperfect crystal for the monomers, but actually creates an amorphous configuration for the dimer centroids [Fig. 1(g)].

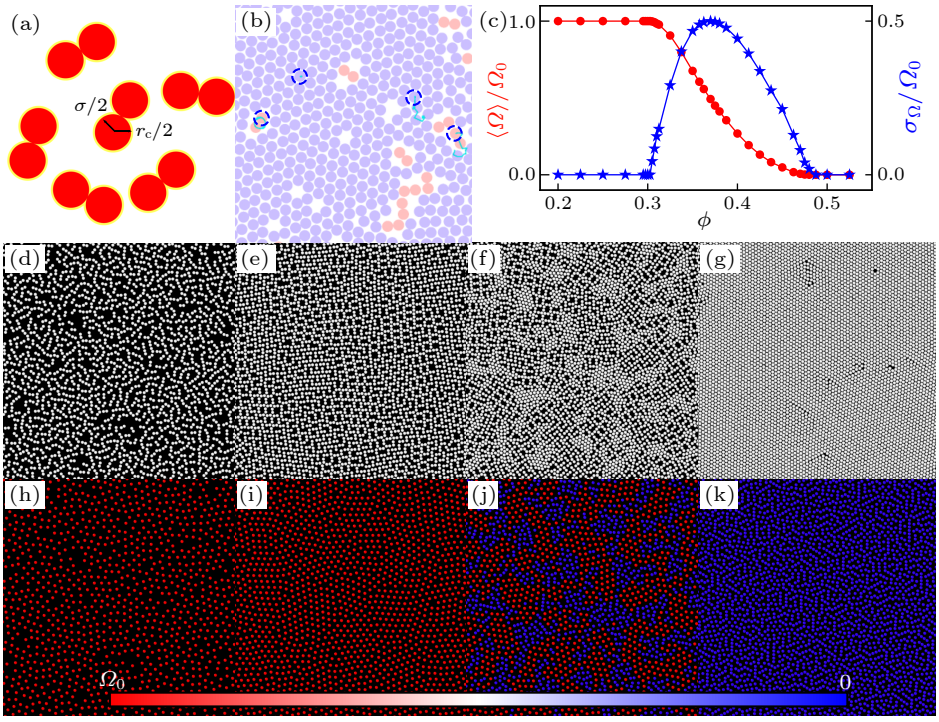

Fig. 1. (a) Simulated dimers with core size σ and interaction distance cutoff r_c. (b) Four types of particle dynamics: monomers circled by blue dashes show different trajectories (cyan), long trajectories indicate diffusion while point/circle trajectories indicate jamming/absorbing, dimers in shaded red rotate freely and those in shaded blue barely rotate. (c) Average angular velocity $\langle\Omega\rangle$ and its standard deviation σ_Ω, as functions of ϕ. (d)–(g) Steady state snapshots for systems at $\phi = 0.2, 0.3, 0.4, 0.5$. (h)–(k) Dimer centroids extracted from (d)–(g), with the spin velocity Ω indicated by colors.

Generally, four typical types of particle dynamics can be observed during the whole procedure, as indicated by blue circles in Fig. 1(b): (1) absorbing but freely spinning, (2) completely jammed, (3) rotationally jammed but diffusing, (4) spinning and diffusing. The former two are respectively the only type of particle dynamics in the ABS and that in the TJS, while all the dynamics can be observed in the intermediate LJS. The local jamming actually leads to a two-phase fluid, and the diffusive dynamics can be observed either near the phase boundaries or in clusters moving as a whole.

The local rotational jamming transition corresponds to a crossover in the averaged angular velocity of all the spinners $\bar{\Omega} = \langle\Omega\rangle/\Omega_0$ (where $\Omega \equiv \dot{\theta}$, and the measure is normalized by the freely spinning velocity $\Omega_0 = \mathcal{T}/\gamma_s$), as shown in Fig. 1(c). In this specific system, the crossover

ranges from a lower transition point at $\phi \approx 0.31$ to a higher one at $\phi \approx 0.48$. Critically at the lower transition point $\phi = 0.31$, cross structures (or T-structures called in Ref. [12]) of freely spinning dimers are observed [Fig. 1(e)]. Due to spin phase differences, the dimers may not interfere with each other, even when their centroids get closer than the dynamical sweeping range $(\sigma + r_c)/2$. Any initial state of the system, with arbitrary overlaps between the dimers' sweeping ranges, would dynamically reorganize and spontaneously generate randomness in the spin phase differences. Such a mechanism automatically avoids crystallization and produces amorphous structures. Around the higher transition point $\phi = 0.48$, a complete jamming trivially leads to a crystal-like structure at the monomer scale, with unavoidable dislocations generated by the self-imposed stresses and the odd elasticity [18] of the jammed spinners.

The local rotational jamming may start from a single dimer, which ceases spinning due to a little bit of overcrowding. As a result of the large relaxation time ratio $\tau_s/\tau_t = 1000$, the dimers tend to separate into distinct spinning and non-spinning regions rather than globally slow down, as the density increases. Since the squeezing occurs homogeneously, the system resembles a microphase-separation process and presents a two-phase morphology, with high-density clusters of $\Omega \approx 0$ in the rotationally jammed regions and freely spinning cross structures of $\Omega \approx \Omega_0$ for the rest. The above features ensure that the crossover corresponding to the transition never gets as sharp as that in Ref. [12].

As angular velocities of the dimers are spontaneously discretized into two values, statistics of Ω automatically measure the number faction of spinners in either phase for the two-phase morphology. The standard deviation of the angular velocity σ_Ω reaches its maximum value $\Omega_0/2$ at about $\phi = 0.37$ [Fig. 1(c)], indicating an equal partition between the two phases, with half free spinners and half rotationally jammed ones. In contrast with the crossover in $\bar{\Omega}$, one observes an abrupt change in σ_Ω at both the lower and higher transition points. The rapid deviation from 0 when ϕ increases from 0.31 or decreases from 0.48 shows that σ_Ω is a better indicator for the local jamming transition.

The system produces disordered patterns for various densities, below or beyond the lower critical point $\phi \approx 0.31$. Even for the TJS beyond the higher critical point $\phi \approx 0.48$, randomness in the orientation of the dimers causes strong disorder in their centroid configurations. Steady-state configurations of the dimer centroids for different states are respectively shown in Figs. 1(h)–1(k), which are obviously disordered as point configurations.

The rich disordered patterns exhibited by the system have different extents of uniformity, as can be seen from Fig. 1. Treated as point configurations, one can measure the density fluctuations $\langle \delta^2 \rho(R) \rangle \equiv \langle \rho^2(R) \rangle - \langle \rho(R) \rangle^2$ for a randomly chosen spherical window with radius R ($R < L/2$ to avoid finite size effect). The analysis can be performed on either the monomers or the dimer centroids, for either all spinners or only the free ones. Here in Fig. 2, we only present the analysis on dimer centroids for all the spinners in the system.

The ABS at a density below the lower critical point (e.g., $\phi = 0.25$ in Fig. 2), shows a density fluctuation suppression, with a vanishing scaling relation $\langle \delta^2 \rho(R) \rangle \sim R^{-2.9}$ extending up to some length scale (about 10σ for $\phi = 0.25$). Such a behavior commonly exists for ABS's of many different systems. [19,20] The length scale diverges as the density approaches the critical value $\phi \approx 0.31$, and the vanishing scaling relation extends to the system size scale (see $\phi = 0.3125$ in Fig. 2). This result evidences that the critical ABS has hyperuniformity properties of almost the strongest class.

The TJS at density beyond the higher critical point (e.g., $\phi = 0.50$ in Fig. 2) has small density fluctuations, which is comparable with the critical hyperuniform case even for large R. However, the large-R asymptotic behavior $\langle \delta^2 \rho(R) \rangle \sim R^{-2}$ indicates that the jammed configuration is intrinsically non-hyperuniform.

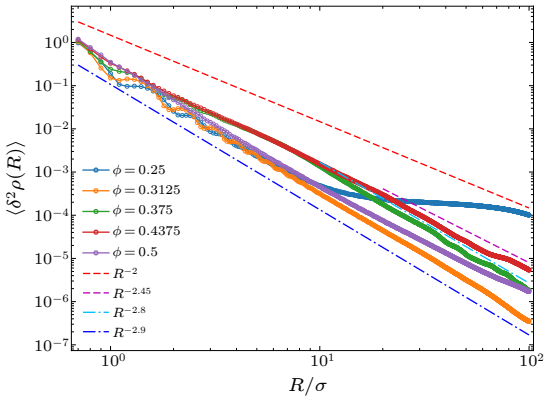

Fig. 2. Density fluctuations $\langle \delta^2 \rho \rangle$ as functions of window size R for various ϕ, measured at fixed system size $L = 400\sigma$. Various lines show different asymptotic $R^{-\alpha}$ scalings.

The LJS corresponding to the crossover has diffusive dynamics, and we naively perform the same analysis for some instantaneous steady-state snapshots. The results for $\phi = 0.375$ and 0.4375 are shown in Fig. 2. For small R, the density fluctuation behavior mimics those of the ABS and the TJS, since statistics are mainly carried out inside one phase and phase boundaries are rarely involved. Beyond some length scale (typically 10σ), a scaling relation $\langle \delta^2 \rho(R) \rangle \sim R^{-\alpha}$ with ϕ-dependent α is observed. Obviously, α varies due to changes of the cluster sizes of either phase. For a finite simulation set, the exponent α measured could be as small as 2.4 (still well beyond the hyperuniformity criterion 2), or as large as 2.9 (close to the strongest hyperuniformity).

To further characterize the disordered hyperuniformity of the system, we calculate the structure factor $S(q)$ for such point configurations of dimer centroids, which are shown in Fig. 3(a). Typically for a hyperuniform system, $S(q) \to 0$ as $q \to 0$, with asymptotic scaling $S(q) \sim q^\beta$ ($\beta > 0$). The $S(q)$ for the subcritical ABS at $\phi = 0.25$

or for the TJS at $\phi = 0.5$ increases as $q \to 0$. These behaviors are consistent with the results of the density fluctuation analysis that the two states are not hyperuniform at large scales. For the critical ABS at $\phi = 0.3125$ and the LJS at $\phi = 0.4$, decays in $S(q)$ are found as $q \to 0$, with scaling relations $S(q) \sim q^{0.6}$ and $\sim q^{1.0}$, respectively.

A hyperuniformity index $H = S(q \to 0)/S_{\text{peak}}$ (where S_{peak} is the peak value) can be defined with the calculated structure factors $S(q)$.[1] Empirically, one has $H \lesssim 10^{-3}$ for hyperuniform configurations.[21,22] We plot the corresponding H as a function of ϕ in red for system of size $L = 400\sigma$ in Fig. 3(b), and more data are shown in blue for a smaller system with $L = 200\sigma$. In both cases, we observe a drastic decrease in H to below 10^{-3} for the critical ABS, indicating a strong hyperuniformity. However, H does not reflect the hyperuniform feature of the LJS, and is a bit misleading for becoming low in the TJS, which is intrinsically not hyperuniform.

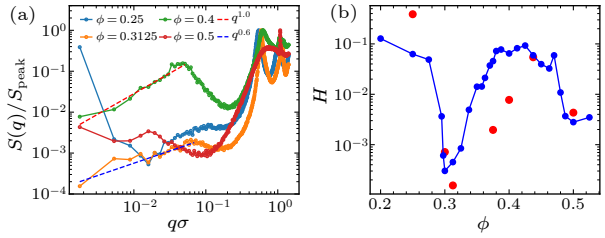

Fig. 3. Structure factor $S(q)$ and hyperuniformity index $H(\phi)$: (a) $S(q)$ at $\phi = 0.25, 0.3125, 0.4, 0.5$ for system size $L = 400\sigma$, the dashed lines show the asymptotic small-q scalings. (b) The corresponding $H(\phi)$ to the system in (a) is shown in red, and much more data for a smaller system ($L = 200\sigma$) is shown in blue for comparison.

To correctly characterize the LJS, we need to treat it as a two-phase media, by thresholding some scalar field. The angular velocity Ω is a pseudo-scalar for a 2D system, one thus can construct a scalar field $\Omega(\boldsymbol{r})$ (see the Supplementary Information for details). With the jammed phase ($\Omega = 0$) and the active phase ($\Omega = \Omega_0$) respectively colored in blue and red, a typical two-phase field for $\phi = 0.375$ is shown in Fig. 4(a).

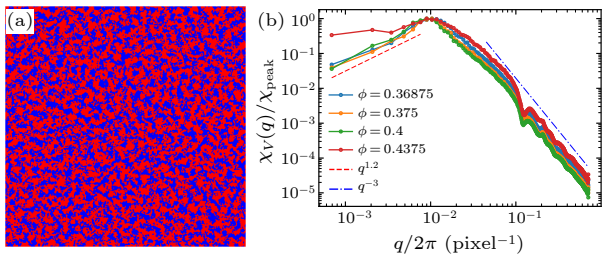

Fig. 4. Two-phase hyperuniformity: (a) the two-phase field $\Omega(\boldsymbol{r})$ for $\phi = 0.375$; (b) the spectral density $\chi_V(q)$ for $\phi = 0.36875, 0.375, 0.4, 0.4375$, the dashed line at small q shows a $q^{1.2}$ law approaching to zero, and the dash-dotted line shows a q^{-3} scaling for large q.

For a hyperuniform two-phase media, its spectral density $\chi_V(q)$ approaches to zero as $q \to 0$, with $\chi_V(q) \sim q^{\gamma}$ ($\gamma > 0$).[1,3] For an image representation with square pixels, the spectral density can be measured as $\chi_V(\boldsymbol{q}) = m^2(\boldsymbol{q})\phi^i S^i(\boldsymbol{q})$,[10,23] where the shape factor $m(\boldsymbol{q}) = \text{sinc}(q_x/2)\text{sinc}(q_y/2)$, ϕ^i is the volume fraction for either phase denoted by the superscript i, and $S^i(\boldsymbol{q})$ is the structure factor for the corresponding pixel centers. We perform the analysis with the active phase data for various LJS's, and the results are shown in Fig. 4(b). Obviously, such two-phase states have a strong-hyperuniformity characteristics with $\gamma > 1$ ($\gamma \approx 1.2$). It is worth noting that all the normalized spectral density curves collapse except for some very large density (e.g., $\phi = 0.4375$). This indicates that the relative phase cluster sizes, which generally change with ϕ, are not critical for hyperuniformity. The system can stably develop hyperuniform morphologies for the two phases with either equal or unequal concentrations. The arbitrary shapes of the clusters also indicate that they possess no effective surface tension. For $\phi = 0.4375$, the small-q scaling seems to have a much smaller γ, possibly due to some statistical reason. As we choose the active phase as the explicit one in all calculations, the number of the spinners involved in this case is quite small since most of them are jammed. Additionally, the system always has a q^{-3} decay at the large q side, which is similar to that of the numerically designed patterns through Fourier-space construction.[10]

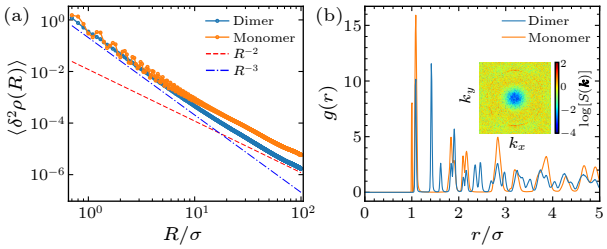

Fig. 5. The TJS at $\phi = 0.5$: (a) density fluctuations $\langle\delta^2\rho(R)\rangle$ for the dimer centroids (blue) and the monomers (orange), in which The dashed and dash-dotted lines respectively show the R^{-2} and R^{-3} scalings; (b) the radial distribution functions $g(r)$ for the dimer centroids (blue) and the monomers (orange), where the inset shows the structural factor $S(\boldsymbol{k})$ for the dimer-centroid configuration.

As it is known that density hyperuniformity is related to incompressibility, the fact that the TJS, which is nearly incompressible, is not hyperuniform, is strange, especially when the monomer configuration appears to be crystal-like. We perform the density-fluctuation analysis for the monomer configurations, which shows more-or-less the same behavior as that of the dimer centroids, with $\sim R^{-3}$ at small R and $\sim R^{-2}$ at large R [see Fig. 5(a)]. We argue that such a behavior is due to some intrinsic constraints within the current system. The monomers form imperfect hexagons as we have $r_c \neq \sigma$, with the radial distribution function $g(r)$ peaking at both $r = \sigma$ and $r = \frac{\sigma + r_c}{2}$ [as shown in Fig. 5(b)]. Random orientations of the dimers leads to a random tiling of the imperfect hexagons, and we have an intrinsic fluctuation proportional to $\frac{r_c - \sigma}{2}$ in determining pair distances. Such a fluctuation is small but independent of the size R of any

window chosen for statistics. Thus, the fluctuation can not be averaged out and always causes a number-counting fluctuation proportional to the peripheral length of the window, i.e., $\sim R^{d-1}$. The fluctuation is negligible for small R, but becomes dominant when the statistical fluctuation vanishes at large R.

More interestingly, the *disordered* dimer-centroid configuration, as the imperfect monomer crystal, also shows sharp peaks in $g(r)$ [Fig. 5(b)], and the corresponding structural factor $S(\boldsymbol{k})$ [inset of Fig. 5(b)] still inherits a six-fold symmetry even though it has been somehow angularly blurred. The $S(\boldsymbol{k})$, without an angular average, approaches zero at many but not all $\boldsymbol{k}$ points in some range like $|\boldsymbol{k}| < K$, which may be viewed as a variant originating from stealthy hyperuniformities.[24–27] These strange features of the TJS indicates that there is still plenty of room in-between ordered and disordered, hyperuniform or nonhyperuniform configurations, and thus are inspiring for designing new materials.

Conclusively, multi-scale disordered hyperuniformities are revealed in a simple active spinner system. The small requirements of the system on particle constitutions and pair interactions are encouraging for fabricating various hyperuniform amorphous structures through dynamical organization.

The critical hyperuniformity in the ABS's of such spinner systems is uncovered for the first time, and is found to belong to almost the strongest class. A novel phenomenon also discovered is the subsequent two-phase hyperuniformity during the local jamming transition, which could also be of a strong class. Additionally, the final TJS, which is intrinsically nonhyperuniform but with confined density fluctuations to a rather low level, may provide ideas for designing interesting nonhyperuniform or even antihyperuniform materials.[28,29]

Though only zero-temperature results are present here, we have carried out some finite temperature simulations. For low temperatures, all the results remain qualitatively the same, as discussed in Ref. [15]. When the temperature becomes high enough, the system goes into the active fluidic regime and a hyperuniform fluid as that in Ref. [17] is recovered.

Active spinner systems are known to break time-reversal symmetry and show topological behaviors.[30–33] We have observed multiple vortices induced by caged diffusion of the free spinners in the two-phase regime, which obviously correspond to spontaneous topological edge flows along spontaneously generated phase boundaries. Furthermore, dislocations are found to inevitably exist due to "odd" stresses of the active spinners in the TJS's.

Acknowledgments. This work was supported by the National Natural Science Foundation of China (Grant Nos. 11774393, 11404378, 12274448, 22272040, and T2325027), Youth Innovation Promotion Association of CAS (Grant No. 2017014), and the National Key R&D Program of China (Grant Nos. 2022YFF0503504 and 2022YFA1203200).

References

[1] Torquato S 2018 *Phys. Rep.* **745** 1
[2] Torquato S and Stillinger F H 2003 *Phys. Rev. E* **68** 041113
[3] Torquato S 2016 *Phys. Rev. E* **94** 022122
[4] Torquato S 2016 *J. Phys.* **28** 414012
[5] Torquato S 2021 *Phys. Rev. E* **103** 052126
[6] Florescu M, Torquato S, and Steinhardt P J 2009 *Proc. Natl. Acad. Sci. USA* **106** 20658
[7] Leseur O, Pierrat R, and Carminati R 2016 *Optica* **3** 763
[8] Froufe-Pérez L S, Engel M, Sáenz J J, and Scheffold F 2017 *Proc. Natl. Acad. Sci. USA* **114** 9570
[9] Gkantzounis G, Amoah T, and Florescu M 2017 *Phys. Rev. B* **95** 094120
[10] Chen D and Torquato S 2018 *Acta. Mater.* **142** 152
[11] Yu S, Qiu C W, Chong Y, Torquato S, and Park N 2021 *Nat. Rev. Mater.* **6** 226
[12] Kirchhoff R and Löwen H 2005 *Europhys. Lett.* **69** 291
[13] van Zuiden B C, Paulose J, Irvine W T, Bartolo D, and Vitelli V 2016 *Proc. Natl. Acad. Sci. USA* **113** 12919
[14] Torquato S 2021 *Proc. Natl. Acad. Sci. USA* **118** e2107276118
[15] Lei Q L, Ciamarra M P, and Ni R 2019 *Sci. Adv.* **5** eaau7423
[16] Huang M J, Hu W S, Yang S Y, Liu Q X, and Zhang H P 2021 *Proc. Natl. Acad. Sci. USA* **118** e2100493118
[17] Lei Q L and Ni R 2019 *Proc. Natl. Acad. Sci. USA* **116** 22983
[18] Scheibner C, Souslov A, Banerjee D, Surówka P, Irvine W T M, and Vitelli V 2020 *Nat. Phys.* **16** 475
[19] Hexner D and Levine D 2015 *Phys. Rev. Lett.* **114** 110602
[20] Zheng Y J, Parmar A D S, and Ciamarra M P 2021 *Phys. Rev. Lett.* **126** 118003
[21] Kim J and Torquato S 2019 *Phys. Rev. E* **99** 052141
[22] Zheng Y J, Li Y W, and Ciamarra M P 2020 *Soft Matter* **16** 5942
[23] Kim J and Torquato S 2021 *Phys. Rev. E* **103** 012123
[24] Zhang G, Stillinger F H, and Torquato S 2015 *Phys. Rev. E* **92** 022119
[25] Ma Z and Torquato S 2017 *J. Appl. Phys.* **121** 244904
[26] DiStasio R A, Zhang G, Stillinger F H, and Torquato S 2018 *Phys. Rev. E* **97** 023311
[27] Torquato S, Zhang G, and Stillinger F H 2015 *Phys. Rev. X* **5** 021020
[28] Torquato S, Kim J, and Klatt M A 2021 *Phys. Rev. X* **11** 021028
[29] Oğuz E C, Socolar J E S, Steinhardt P J, and Torquato S 2019 *Acta Cryst. A* **75** 3
[30] Dasbiswas K, Mandadapu K K, and Vaikuntanathan S 2018 *Proc. Natl. Acad. Sci. USA* **115** E9031
[31] Banerjee D, Souslov A, Abanov A G, and Vitelli V 2017 *Nat. Commun.* **8** 1573
[32] Yang Q, Zhu H, Liu P, Liu R, Shi Q, Chen K, Zheng N, Ye F, and Yang M 2021 *Phys. Rev. Lett.* **126** 198001
[33] Yang Q, Liang H, Liu R, Chen K, Ye F, and Yang M 2021 *Chin. Phys. Lett.* **38** 128701